Electronic Supplementary Material (ESI) for Nanoscale.

Ultrasensitive and Highly Stretchable Fiber with Dual Conductive Microstructural Sheaths for Human Motion Sensing and Micro Vibration Sensing

Jieyu Xiao,[ab] Yan Xiong, [ab] Juan Chen, [ab] Shanshan Zhao, [ab] Shangbi Chen, [abcd] Banglian Xu, [ab] Bin Sheng[ab]*

[a] School of Optical Electrical and Computer Engineering, University of Shanghai for Science and Technology, Shanghai 200093, China.

[b] Shanghai Key Laboratory of Modern Optical Systems, Engineering Research Center of Optical Instruments and Systems, Shanghai 200093, China

[c] Shanghai Aerospace Control Technology Institute, Shanghai, 200233, China

[d] Shanghai Xin Yue Lian Hui Electronic Technology Co. LTD, Shanghai, 200233, China

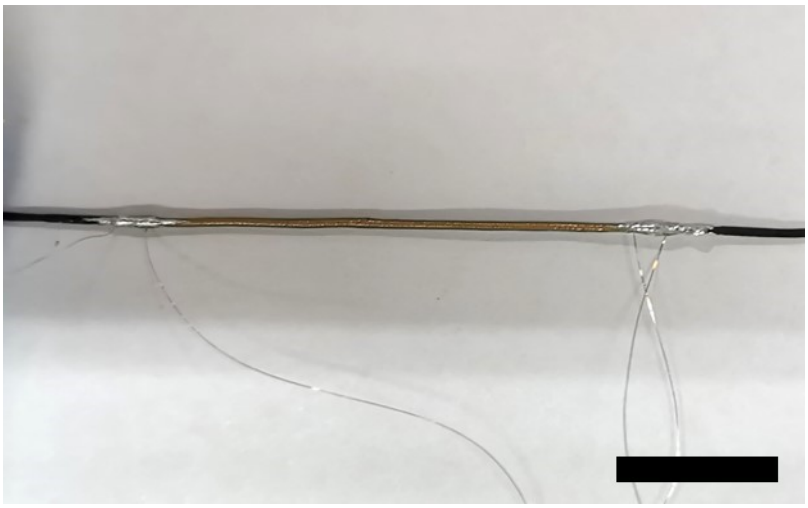

Figure S1. Digital photograph of the DCSF strain sensor. Scale bar represents 10 mm.

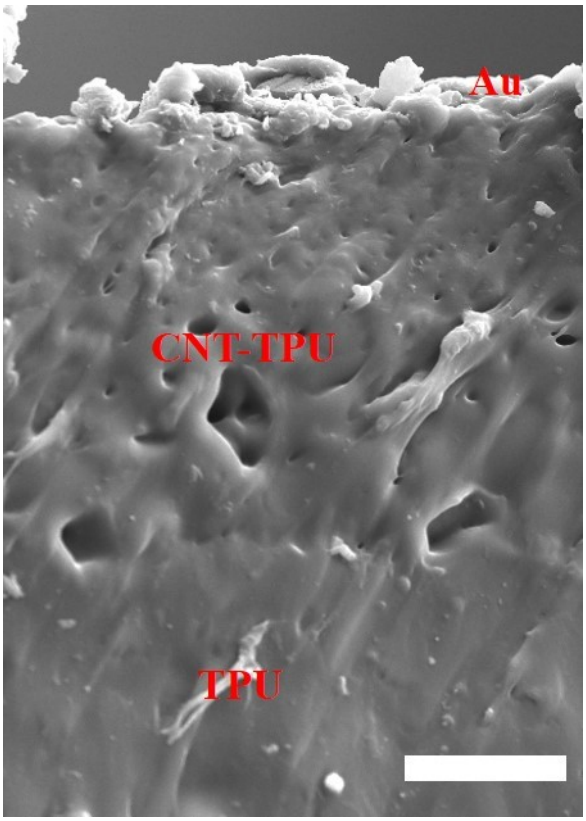

Figure S2. Cross-sectional SEM images of the DCSF. Scale bar represents 10μm.

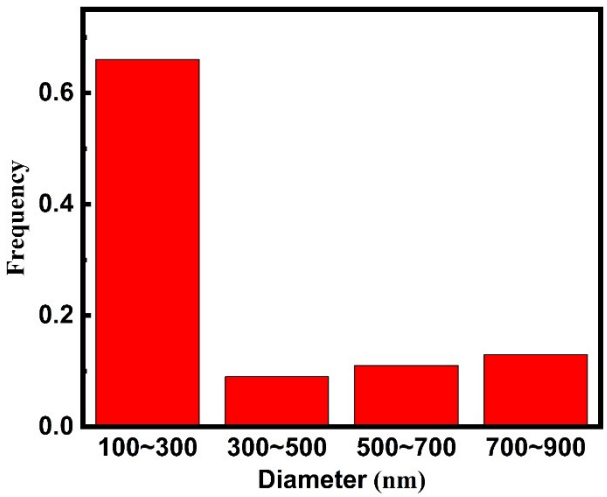

Figure S3 The distribution of the micro-pore in the TPU sheath.

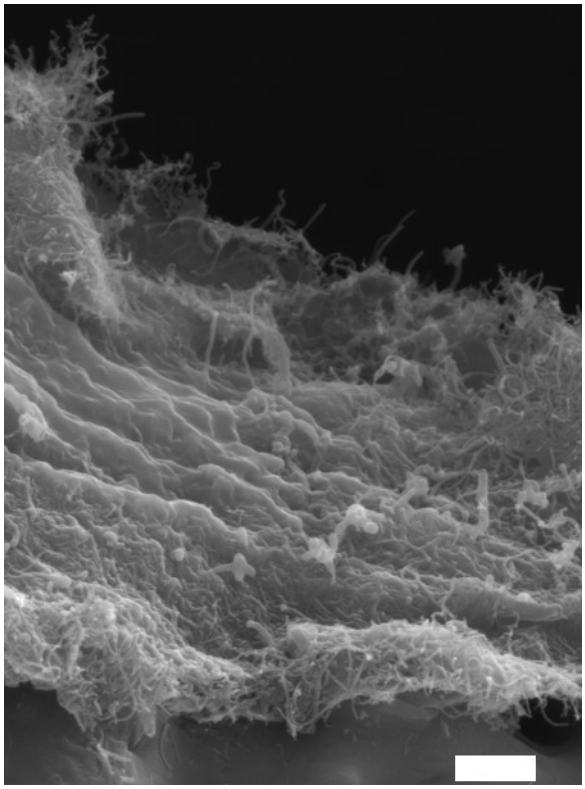

Figure S4. Cross-sectional image of CNT-TPU layer in fracture state. Scale bar represents 1 µm.

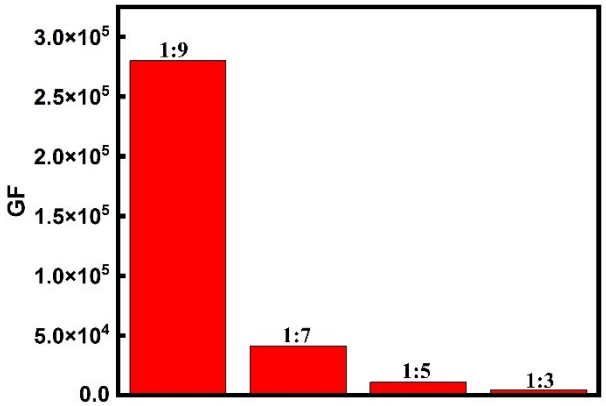

Figure S5. Sensor GF value at the 0-100% stretch range under different CNT ratio.

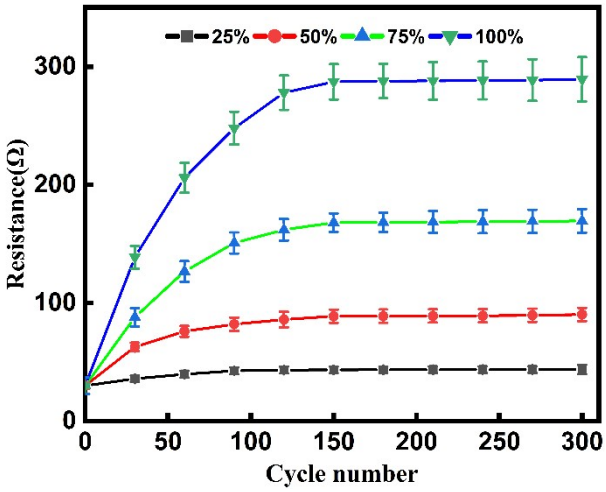

Figure S6 The initial resistance value of DCSF changes with the number of stretches.

Figure S6 shows the relationships between the number of training cycles and the average value of resistance, the average resistance value of the sample stabilized during at least 150 training cycles. The gold film will undergo fatigue fracture due to the stress concentration under the cyclic strain loading, therefore, the relative resistance drift is caused by the increase in the resistance of the sample. So the DCSF strain sensors were all trained for 150 cycles

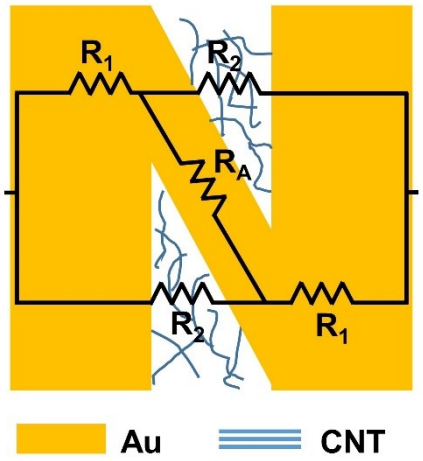

Figure S7 Electrical circuit model of the DCSF.

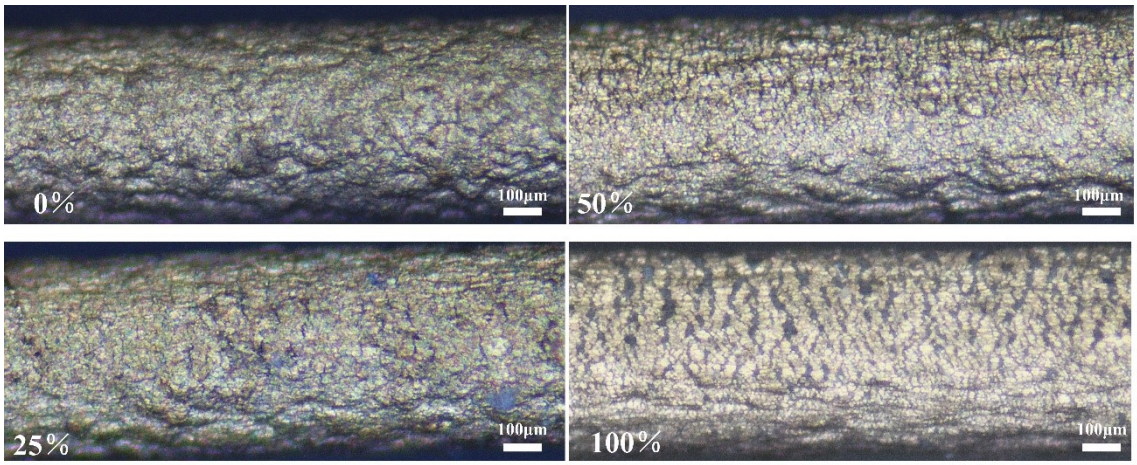

Figure S8 Morphology changes of the DCSF under stretching strain from 0 to 100%.

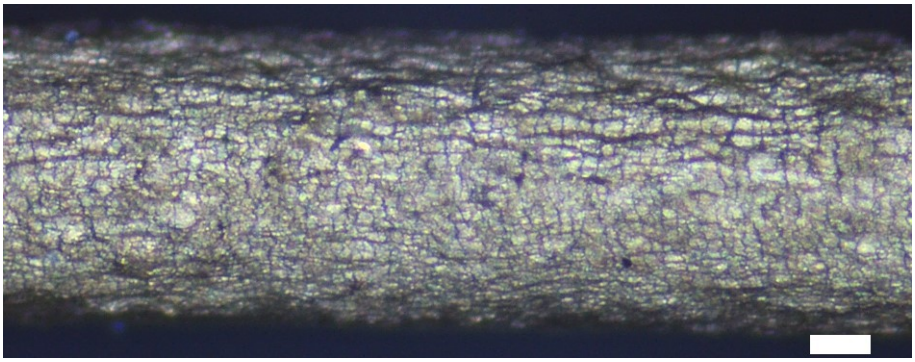

Figure S9. Optical microscope image of the images of the gold film on the porous TPU sheath with the applied strain of 30%. Scale bar represents 100 µm.

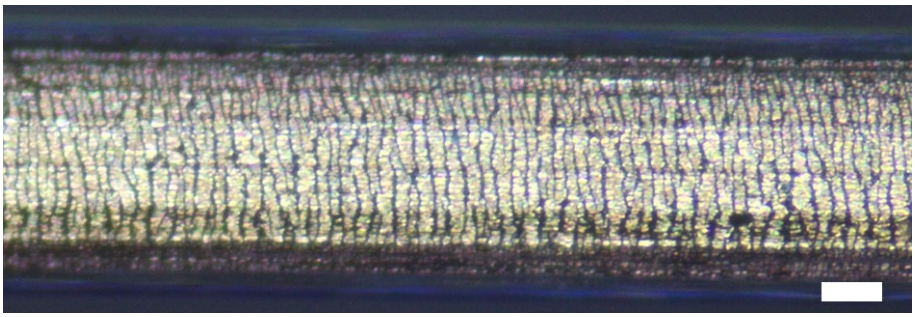

Figure S10. Optical microscope image of the gold film deposited on smooth TPU fiber with the applied strain of 30%. Scale bar represents 100 µm.

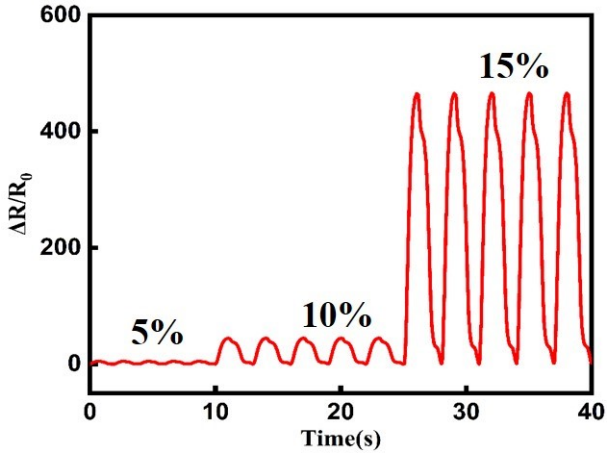

Figure S11 Response of DCSF strain sensor to stepwise cyclic loadings at strains.

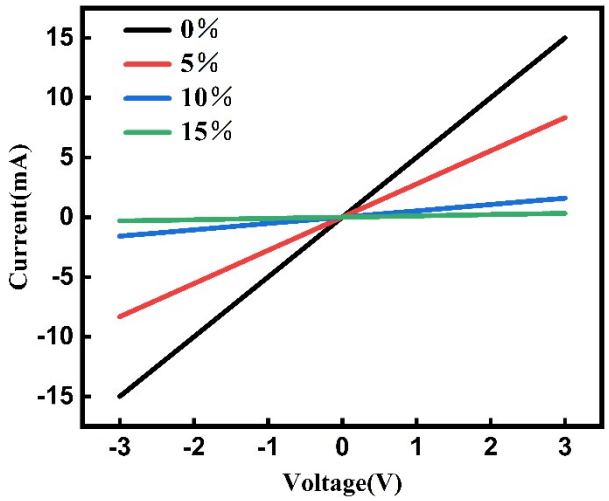

Figure S12 Voltage-current curve under different strains (0, 5, 10 and 15%) for the DCSF strain sensor.

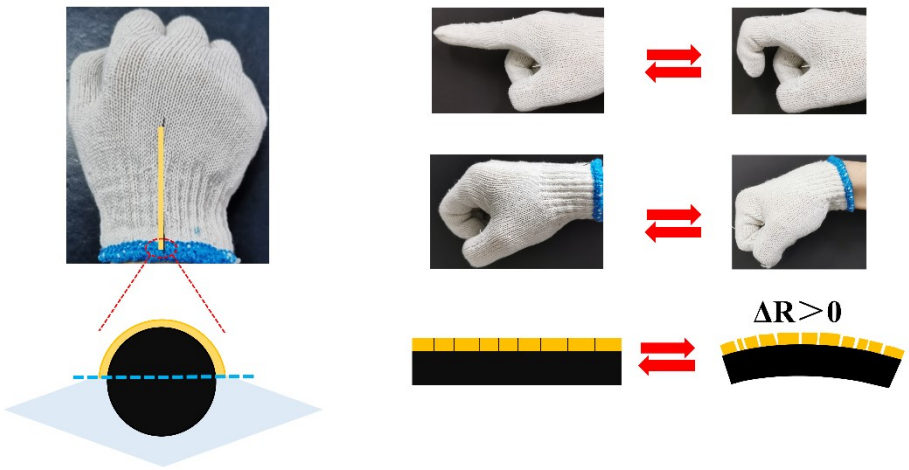

Figure S13. Illustration of the cracks changing in quasi-hemispherical gold sheath located parallel to the back side of the smart sensing glove, while bending of a finger or a wrist.

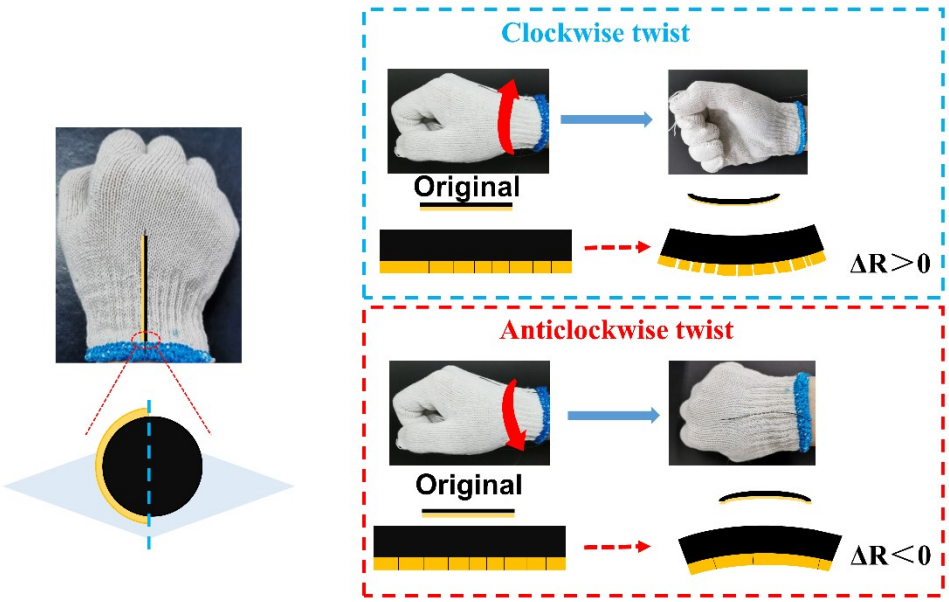

Figure S14. Illustration of the cracks changing in quasi-hemispherical gold sheath located perpendicular to the back side of the smart sensing glove, while twisting of a wrist clockwise or anticlockwise.

Real-time monitoring of repetitive bending of the wrist wearing a glove sewed with our DCSF (Movie S1)

Real-time monitoring of the clockwise and anticlockwise twisted motions of the wrist wearing a glove sewed with our DCSF (Movie S2)

DCSF strain sensor placed on the radial artery by medical adhesive tape to noninvasively monitor the pulse in the relaxation state (Movie S3)

DCSF interconnects with LED for intelligent switch (Movie S4)

Table S1. The summary of fiber strain sensors reported in recent years

Fiber strain sensors	Gauge factor	Workable strain range	References
Carbon hybrid fiber	1127	3.1%	1
Alternate Segmental fiber	23800	30%	2
TPU-CB@TPU fiber	28084	200%	3
SEBs/CNTs filaments	71.76	120%	4
PU/AgNW fibers	3051	43%	5
CNT-based core-sheath fiber	1378	300%	6
CNTs-TPU composite fiber	97.1	320%	7
CNTs-decorated TPU fiber	102	300%	8
CNTs ink/PU yarn	1344.1	200%	9
CPC@PU yarn	39	1%	10
GNSs/Au/GNSs PU yarn	661.59	50%	11
Carbonized Silk fabric	37.5	500%	12
SWNT/MWNT/TPU yarn	1.24	100%	13
TPE-wrapped SWCNT fiber	425	100%	14
SBS/CNT fiber	2889	267%	15
DCSF	**412000**	**100%**	**This work**

REFERENCES:

1 Hu, Y.; Huang, T.; Zhang, H.; Lin, H.; Zhang, Y.; Ke, L.; Cao, W.; Hu, K.; Ding, Y.; Wang, X.; Rui, K.; Zhu, J.; Huang, W., *ACS Applied Materials & Interfaces* **2021**, *13*(20), 23905-23914

2 Jia, J.; Pu, J.-H.; Liu, J.-H.; Zhao, X.; Ke, K.; Bao, R.-Y.; Liu, Z.-Y.; Yang, M.-B.; Yang, W., *Materials Horizons* **2020**, *7* (9), 2450-2459.

3 Yue, X.; Jia, Y.; Wang, X.; Zhou, K.; Zhai, W.; Zheng, G.; Dai, K.; Mi, L.; Liu, C.; Shen, C., *Composites Science and Technology* **2020**, *189*(35), 108308.

4 Cui, X.; Jiang, Y.; Xu, Z.; Xi, M.; Jiang, Y.; Song, P.; Zhao, Y.; Wang, H., *Composites Part B: Engineering* **2021**, *211*(9), 108641.

5 Zhu, G. J.; Ren, P. G.; Guo, H.; Jin, Y. L.; Yan, D. X.; Li, Z. M., *ACS Applied Materials & Interfaces* **2019**, *11* (26), 23649-23658.

6 Tang, Z.; Jia, S.; Wang, F.; Bian, C.; Chen, Y.; Wang, Y.; Li, B., *ACS Applied Materials & Interfaces* **2018**, *10* (7), 6624-6635.

7 Wang, X.; Sun, H.; Yue, X.; Yu, Y.; Zheng, G.; Dai, K.; Liu, C.; Shen, C., *Composites Science and Technology* **2018**, *168*, 126-132.

8 Yu, Y.; Zhai, Y.; Yun, Z.; Zhai, W.; Wang, X.; Zheng, G.; Yan, C.; Dai, K.; Liu, C.; Shen, C., *Advanced Electronic Materials* **2019**, *5* (10), 1900538.

9 Sun, H.; Dai, K.; Zhai, W.; Zhou, Y.; Li, J.; Zheng, G.; Li, B.; Liu, C.; Shen, C., *ACS Applied Materials & Interfaces* **2019**, *11* (39), 36052-36062.

10 Wu, X.; Han, Y.; Zhang, X.; Lu, C., *ACS Applied Materials & Interfaces* **2016**, *8* (15), 9936-9945.

11 Li, X.; Koh, K. H.; Farhan, M.; Lai, K. W. C., *Nanoscale* **2020**, *12* (6), 4110-4118.

12. Wang, C.; Li, X.; Gao, E.; Jian, M.; Xia, K.; Wang, Q.; Xu, Z.; Ren, T.; Zhang, Y., *Advnced Materials* **2016**, *28* (31), 6640-6648.

13 Li, Y.; Zhou, B.; Zheng, G.; Liu, X.; Li, T.; Yan, C.; Cheng, C.; Dai, K.; Liu, C.; Shen, C.; Guo, Z., *Journal of Materials Chemistry C* **2018**, *6* (9), 2258-2269.

14 Zhou, J.; Xu, X.; Xin, Y.; Lubineau, G., *Advanced Functional Materials* **2018**, *28* (16), 1705591.

15 Yu, S.; Wang, X.; Xiang, H.; Zhu, L.; Tebyetekerwa, M.; Zhu, M., *Carbon* **2018**, *140*, 1-9.